Table 1. GRNs built in this study.

Network type	Study	Note	N	Network label	*TFs**	*Targets**
Tissue	Chen et al. 2014	B73	53	Chen2014 B73 [53]	1,213	18,136
	Stelpflug et al. 2016	B73	93	Stelpflug2016 B73 [93]	1,447	20,011
	Walley et al. 2016	B73	23	Walley2016 B73 [23]	1,392	19,661
	Zhou et al. 2018	B73	23	Zhou2018 B73 [23]	1,477	19,835
		Mo17	23	Zhou2018 Mo17 [23]	1,472	19,969
		BxM	23	Zhou2018 BxM [23]	1,514	20,364
	Yi et al. 2019	seed dev	31	Yi2019 seed dev [31]	1,142	16,987
	Tissue Atlas	combined	247	Tissue Atlas combined [247]	1,429	20,902
Genotype	Eichten et al. 2013	seedling_leaf3	62	Eichten2013 seedling_leaf3 [62]	1,030	17,993
	Fu et al. 2013	kernel	368	Fu2013 kernel [368]	1,194	19,248
	Hirsch et al. 2014	seedling	503	Hirsch2014 seedling [503]	1,324	20,602
	Leiboff et al. 2015	SAM	383	Leiboff2015 SAM [383]	1,313	20,730
	Lin et al. 2017	ear	26	Lin2017 ear [26]	1,199	19,100
		root	27	Lin2017 root [27]	1,182	20,475
		shoot	27	Lin2017 shoot [27]	1,237	20,665
		tassel	26	Lin2017 tassel [26]	1,208	20,882
		SAM	27	Lin2017 SAM [27]	1,064	18,407
	Kremling et al. 2018	GRoot	201	Kremling2018 GRoot [201]	984	17,359
		GShoot	271	Kremling2018 GShoot [271]	1,030	17,577
		Kern	226	Kremling2018 Kern [226]	893	17,220
		L3Base	254	Kremling2018 L3Base [254]	978	17,431
		L3Tip	257	Kremling2018 L3Tip [257]	995	18,681
		LMAD	199	Kremling2018 LMAD [199]	902	17,823
		LMAN	249	Kremling2018 LMAN [249]	902	17,445
	Shaefer et al. 2018	root_GCN	48	Shaefer2018 root_GCN [48]	1,253	20,593
	Huang et al. 2018	leaf	394	Huang2018 leaf [394]	1,314	20,258
		root	176	Huang2018 root [176]	1,359	20,437
		SAM	406	Huang2018 SAM [406]	1,307	20,310
		seed	159	Huang2018 seed [159]	1,271	19,033
	Mazaheri et al. 2019	seedling	453	Mazaheri2019 seedling [453]	1,329	20,474
	Li et al. 2019	endosperm	121	Li2019 endosperm [121]	778	16,347
		internode	77	Li2019 internode [77]	960	17,820
		leaf	84	Li2019 leaf [84]	915	17,698
		root	84	Li2019 root [84]	1,153	19,221
		shoot	85	Li2019 shoot [85]	1,108	18,648
		seedling	169	Li2019 seedling [169]	1,188	19,264
Tissue*Genotype	Lin et al. 2017	5 tissues	133	Lin2017 5 tissues [133]	1,460	22,387
	Kremling et al. 2018	7 tissues	1,657	Kremling2018 7 tissues [1657]	1,117	19,491
	Huang et al. 2018	4 tissues	1,136	Huang2018 4 tissues [1136]	1,530	21,832
	Zhou et al. 2018	B+M+F1	73	Zhou2018 B+M+F1 [73]	1,499	20,905
	Li et al. 2019	6 tissues	620	Li2019 6 tissues [620]	1,302	20,779
RIL	Li et al. 2013	B73 x Mo17	107	Li2013 B73 x Mo17 [107]	1,095	16,583
	Baute et al. 2016	MAGIC	102	Baute2016 MAGIC [102]	1,055	18,086
	Baute et al. 2015	B73 x H99	106	Baute2015 B73 x H99 [106]	1,046	16,798
	Wang et al. 2018	W22 x Teosinte	617	Wang2018 W22 x Teosinte [617]	1,135	17,629

* Top 100,000 predictions

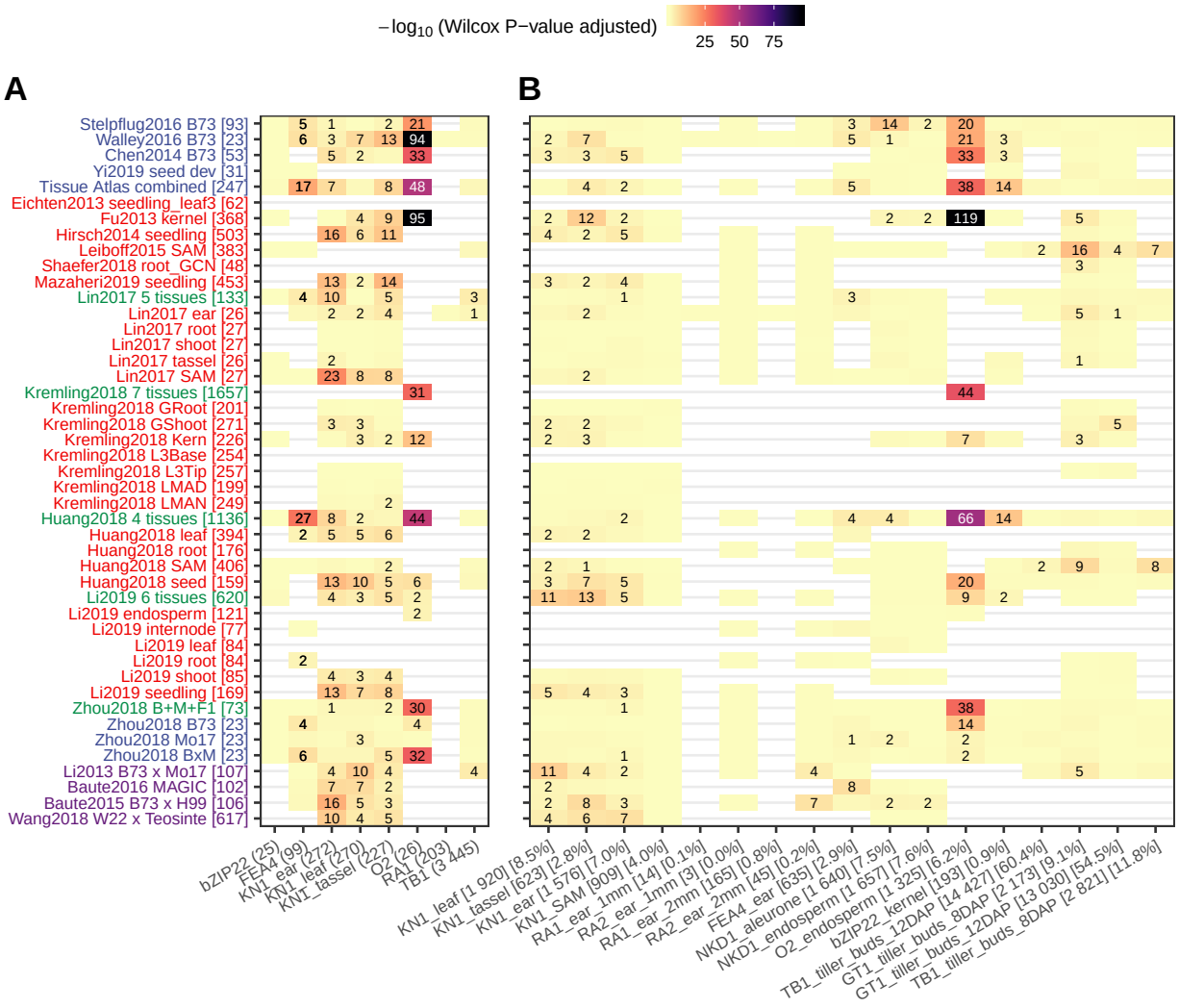

Figure 1. TF-target interactions predicted by GRNs are supported by (A) experimentally derived TF targets and (B) knockout mutant RNA-Seq experiments. (A) direct targets of published TF studies derived from ChIP-Seq and mutant RNA-Seq experiments; (B) For each one of the 17 maize TFs with knockout mutant RNA-Seq data available, differentially expressed genes between mutant and wildtype were identified using DESeq2 (p-value < 0.01). Wilcox rank test were then performed using the predicted (TF-target) interaction scores (top 100k edges) between the group of true targets (DEGs) and non-targets (non-DEGs). P-values were adjusted by the Benjamini-Hochberg method implemented in R. Numbers in each cell show the adjusted test P-value (-log10 transformed) Figure S2 provides the actual number of true targets captured by each GRN during each evaluation. Light yellow cells with no numbers indicate "not significant" (P > 0.05), while blank (white) cells indicate missing data where the TF being evaluated is not expressed or not variable (i.e., zero variance) in the corresponding GRN. Y-axis labels correspond to the different networks listed in Table 1. X-axis labels (e.g., "KN1_ear (272)" or "KN1_ear [1576] [7.0%]") represent the common name for each TF, the tissue in which the TF is expressed, followed by the number of direct targets (Panel A) or number and proportion of differentially expressed genes in TF mutant (Panel B).

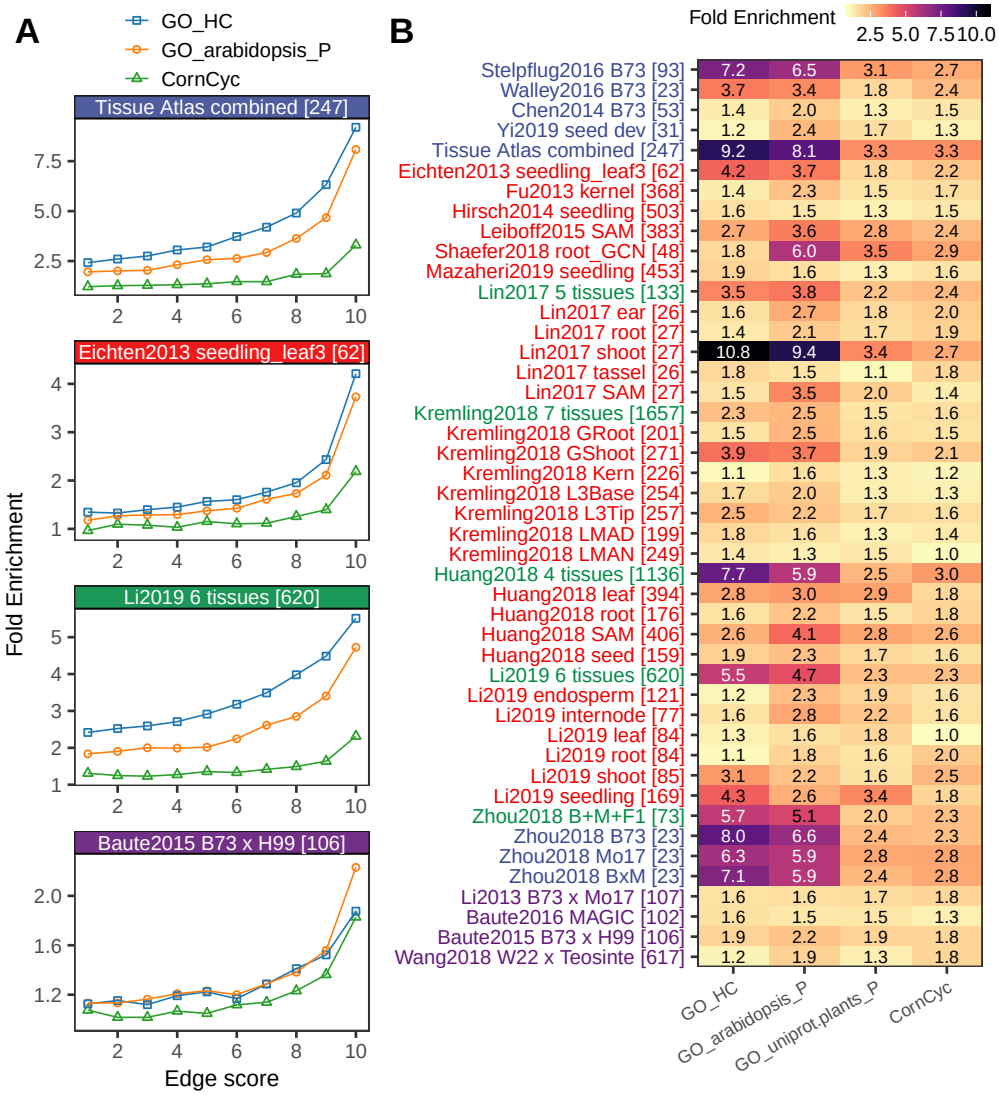

Figure 2. Enrichment of co-annotated GO/CornCyc terms in co-regulated network targets. For each network the top 1 million predicted TF-target associations were binned to 10 bins and assessed for enrichment of GO/CornCyc functional annotation. Fold enrichment is calculated as the observed number of shared GO/CornCyc terms (by targets regulated by a common TF) divided by the expected number of shared annotation terms (determined by permutation). (A) GO/CornCyc enrichment is shown for 4 selected networks. (B) Heatmap showing enrichment of co-annotated GO/CornCyc terms in the first bin (i.e., top 100k) of edges in the GRNs. See Figure S7 for the enrichment in all bins of all built GRNs. A total of six sources of GO annotation were used but only three were shown here: GO_HC (high quality hand-curated terms transferred from maize AGP_v3 annotation), GO_arabidopsis and GO_uniprot.plants (check Figure S6 for a complete list).

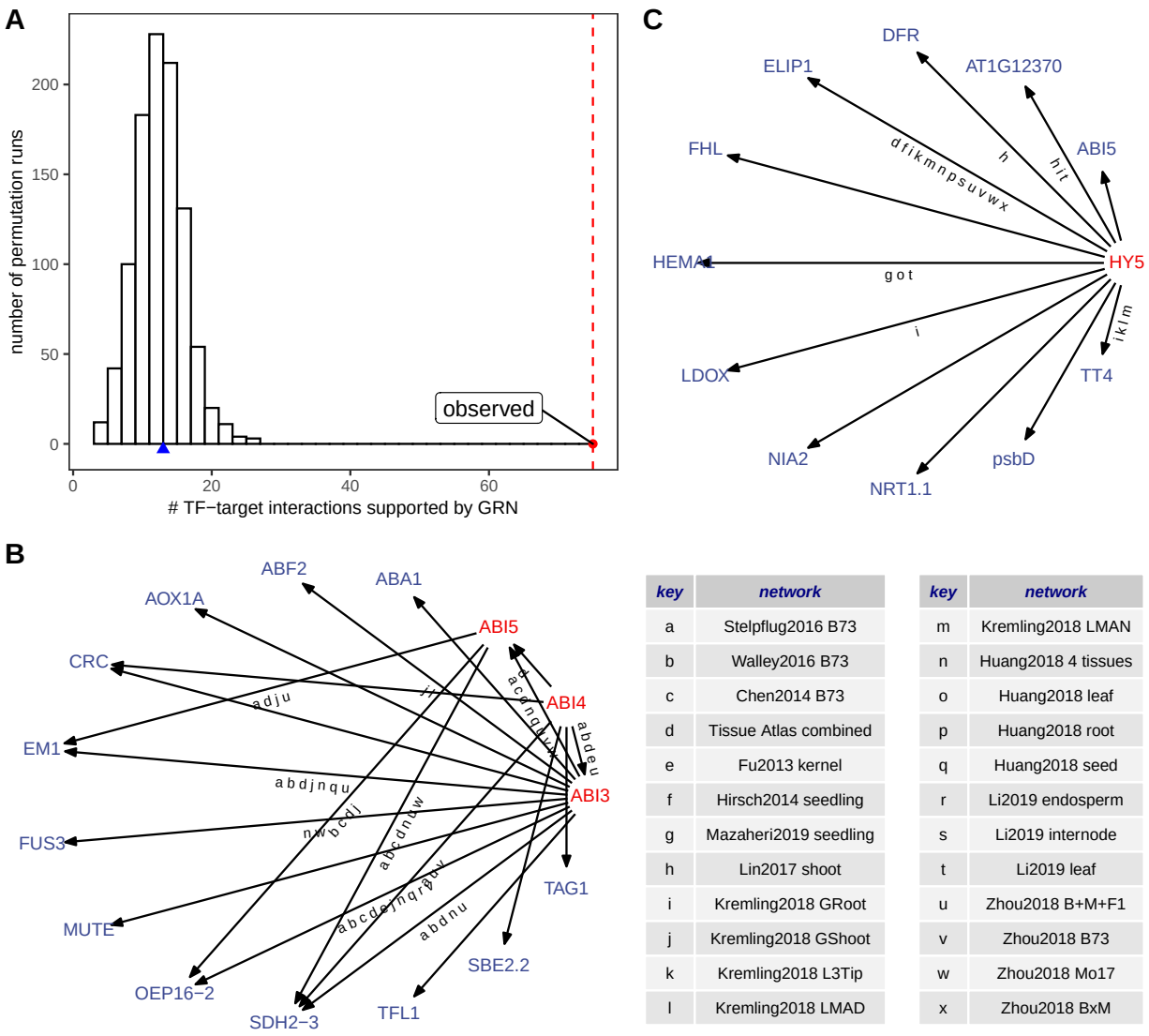

key	network
a	Stelpflug2016 B73
b	Walley2016 B73
c	Chen2014 B73
d	Tissue Atlas combined
e	Fu2013 kernel
f	Hirsch2014 seedling
g	Mazaheri2019 seedling
h	Lin2017 shoot
i	Kremling2018 GRoot
j	Kremling2018 GShoot
k	Kremling2018 L3Tip
l	Kremling2018 LMAD

key	network
m	Kremling2018 LMAN
n	Huang2018 4 tissues
o	Huang2018 leaf
p	Huang2018 root
q	Huang2018 seed
r	Li2019 endosperm
s	Li2019 internode
t	Li2019 leaf
u	Zhou2018 B+M+F1
v	Zhou2018 B73
w	Zhou2018 Mo17
x	Zhou2018 BxM

Figure 3. GRN predictions show enrichment of documented transcriptional regulations from Arabidopsis. (A) Permutation analysis showing the number of random TF-target interactions supported by at least one of the 45 GRNs (histogram) as compared to the actual regulations (transferred from Arabidopsis) with GRN support (red dashed line). (B) The abscisic acid (ABA) pathway transferred from Arabidopsis showed support for 12 out of the 20 edges. (C) 6 out of the 11 HY5 (Elongated Hypocotyl 5) targets transferred from Arabidopsis showed support in at least one GRN. The letters along the edges of the networks in (B) and (C) indicate significant support from specific GRN as indicated in the key.

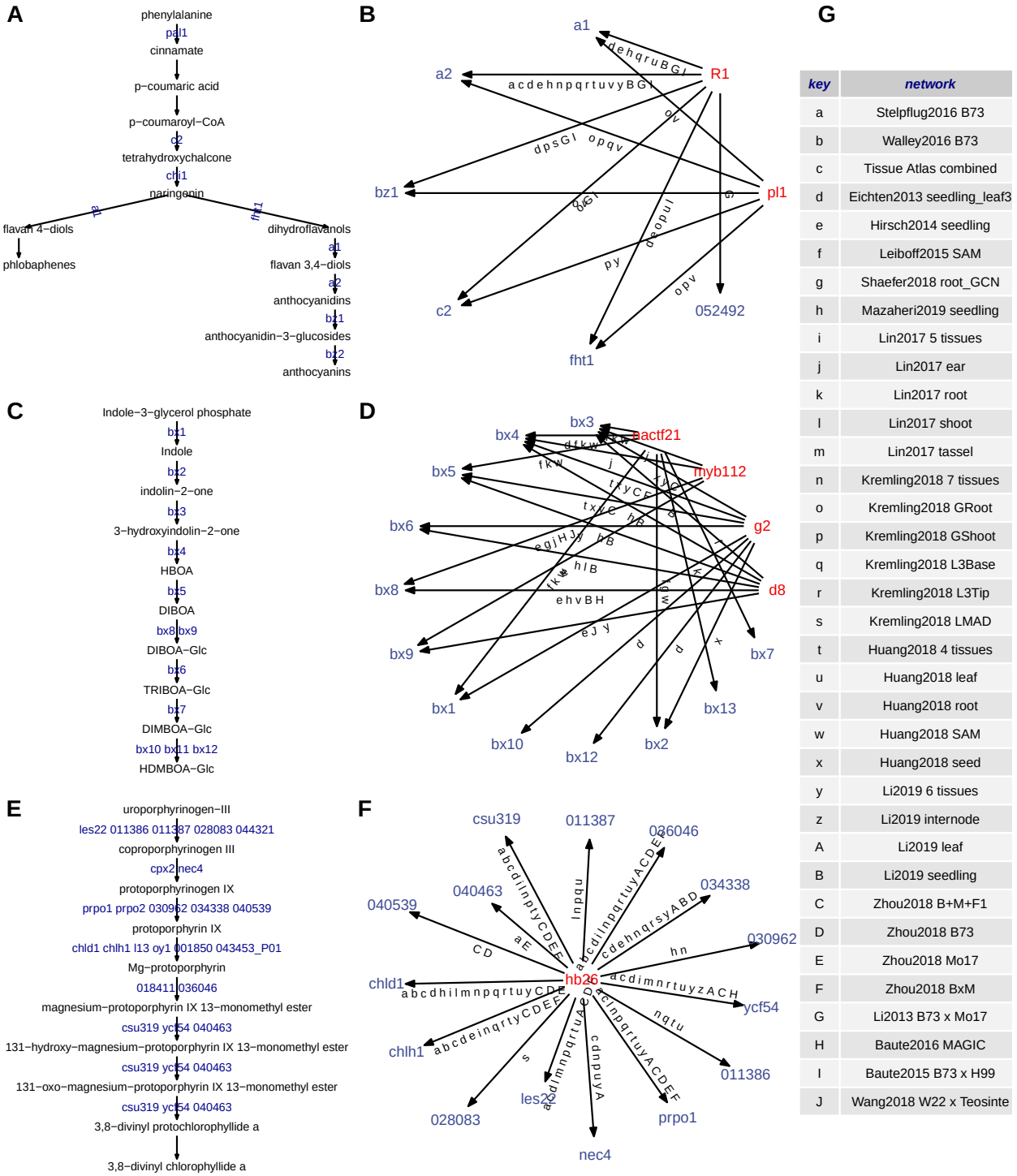

key	network
a	Stelpflug2016 B73
b	Walley2016 B73
c	Tissue Atlas combined
d	Eichten2013 seedling_leaf3
e	Hirsch2014 seedling
f	Leiboff2015 SAM
g	Shaefer2018 root_GCN
h	Mazaheri2019 seedling
i	Lin2017 5 tissues
j	Lin2017 ear
k	Lin2017 root
l	Lin2017 shoot
m	Lin2017 tassel
n	Kremling2018 7 tissues
o	Kremling2018 GRoot
p	Kremling2018 GShoot
q	Kremling2018 L3Base
r	Kremling2018 L3Tip
s	Kremling2018 LMAD
t	Huang2018 4 tissues
u	Huang2018 leaf
v	Huang2018 root
w	Huang2018 SAM
x	Huang2018 seed
y	Li2019 6 tissues
z	Li2019 internode
A	Li2019 leaf
B	Li2019 seedling
C	Zhou2018 B+M+F1
D	Zhou2018 B73
E	Zhou2018 Mo17
F	Zhou2018 BxM
G	Li2013 B73 x Mo17
H	Baute2016 MAGIC
I	Baute2015 B73 x H99
J	Wang2018 W22 x Teosinte

Figure 4. Different coexpression-based GRNs capture distinct aspects of classic and CornCyc metabolic pathways. (A-B) The anthocyanin biosynthesis pathway (A) regulated by R1 (Zm00001d026147) and pl1 (Zm00001d037118). (C-D) The DIMBOA biosynthesis pathway (C) and four potential regulators (D): g2 (Zm00001d039260), d8 (Zm00001d033680), nactf21 (Zm00001d036050) and myb112 (Zm00001d046632). (E-F) The chlorophyllide biosynthesis pathway (E) potentially regulated by hb26 (Zm00001d008612) (F). (G) Network key mappings used in panels (B) (D) and (F). Mappings of reference gene IDs to aliases were obtained from MaizeGDB (https://maizegdb.org/associated_genes?type=all&style=table). For genes with-

out aliases the reference gene ID were prefix-trimmed (“Zm00001d”) before displaying.

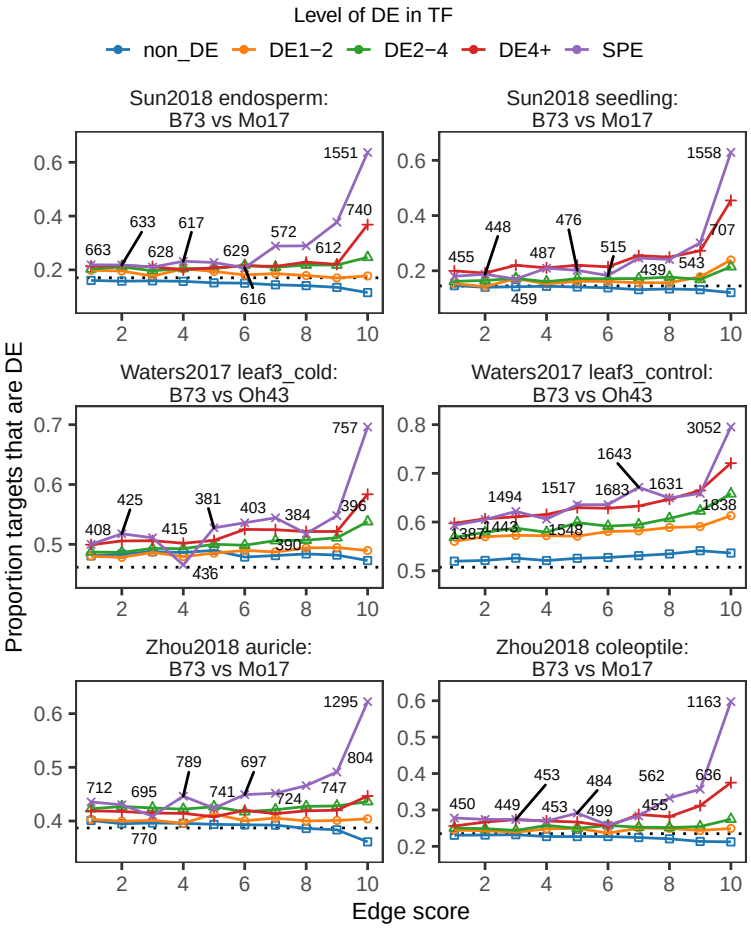

Figure 5. TF-target validation of the combined tissue network in three selected natural variation datasets. Each panel shows the proportion of differentially expressed targets regulated by TFs showing different DE levels between two genotypes in one tissue/treatment condition. For each network the top 1 million TF-target predictions were binned to 10 groups based on the interaction score in GRN. Each TF-target pair is classified according to the DE level of the TF ("non_DE", "DE1-2", "DE2-4", "DE4+" or "SPE") in each network. The proportion of TF-target pairs with the target also showing DE was then determined for each category. Dashed line in each panel represents the genome-wide (background) proportion of DE genes in each tissue/treatment setting.

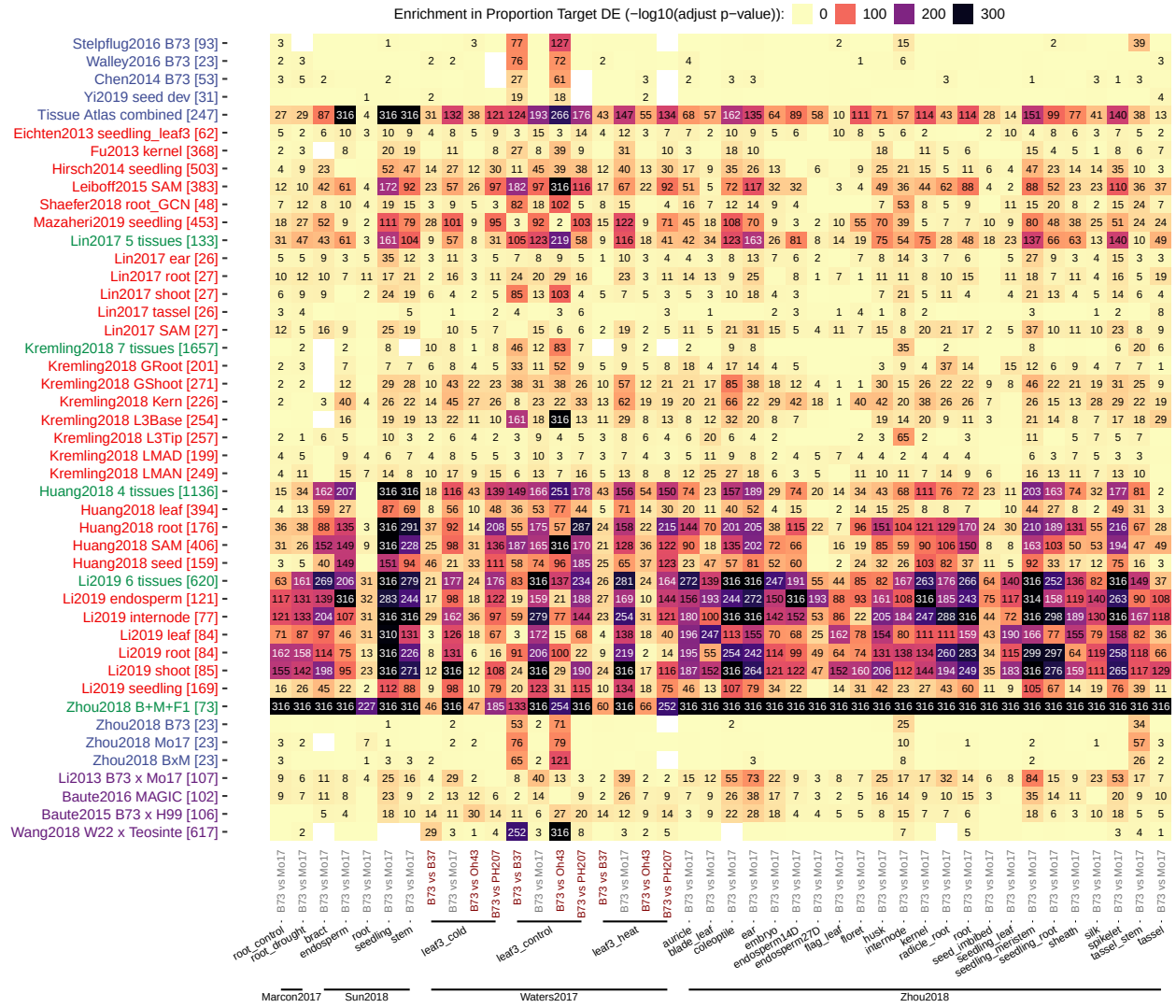

Figure 6. Enrichment in differentially expressed targets regulated by TFs that show SPE patterns. Color and number in each cell represents the enrichment P-value (-log10 transformed, Benjamin-Hhochberg adjusted hypergeometric test p-value) of (SPE TF regulated) target DE proportions relative to the genome-wide proportion of DEGs for each GRN (row-wise) evaluated against a tissue/treatment condition in a natural variation dataset (column-wise). Only edges in the first bin (top 100k) of each network were taken.

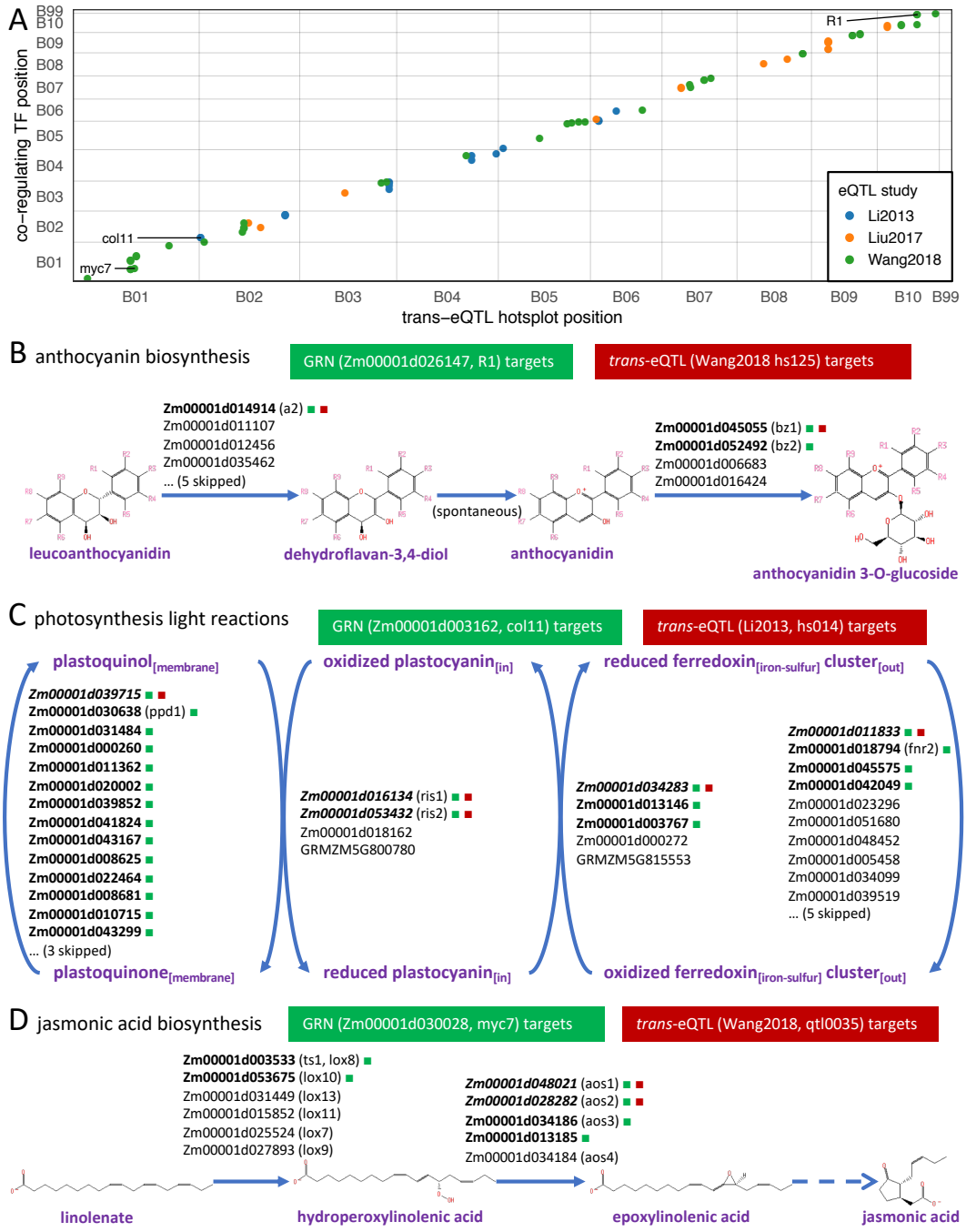

Figure 7. Identification of acting transcription factors underlying trans-eQTL hotspots identified in previous studies. (A) Co-localization of TFs predicted by GRNs in this study and trans-eQTL hotspots identified in previous studies that regulate the same set of targets. Each dot represents a TF supported by at least two high quality networks to show significant co-regulation with at least one trans-eQTL hotspot, and are within 50-Mbp distance from the trans-eQTL hotspot location; (B)-(D) Identification of R1 (Zm00001d026147), col11 (Zm00001d003162) and myc7 (Zm00001d030028) co-localizing previous trans-eQTL hotspots and acting as the master regulator of maize anthocyanin biosynthesis pathway, photosynthesis light reaction pathway and jasmonic acid biosynthesis pathway, respectively.